Elastic and inelastic collisions of ^{6}Li atoms in magnetic and optical traps

M. Houbiers,[1] H. T. C. Stoof,[1] W. I. McAlexander,[2] and R. G. Hulet[2]

[1]*Institute for Theoretical Physics, University of Utrecht, Princetonplein 5, 3584 CC Utrecht, The Netherlands*

[2]*Physics Department and Rice Quantum Institute, Rice University, Houston, Texas 77251-1892*

(Received 30 October 1997)

We use a full coupled-channels method to calculate collisional properties of magnetically or optically trapped ultracold ^{6}Li. The magnetic-field dependence of the s-wave scattering lengths of several mixtures of hyperfine states are determined, as are the decay rates due to exchange collisions. In one case, we find Feshbach resonances at $B=0.08$ T and $B=1.98$ T. We show that the exact coupled-channels calculation is well approximated over the entire range of magnetic fields by a simple analytical calculation. [S1050-2947(98)50703-2]

PACS number(s): 32.80.Pj, 03.75.Fi, 67.40.−w, 42.50.Vk

The observation of Bose-Einstein condensation in atomic alkali-metal gases [1–3] has triggered an enormous interest in degenerate atomic gases. At present, one of the most important goals is to achieve quantum degeneracy in a fermionic gas. In the case of fermionic ^{6}Li, it has been shown theoretically that a BCS transition to a superfluid state could be realized at a critical temperature on the order of temperatures obtained in the BEC experiments [4]. This relatively high critical temperature is due to the fact that ^{6}Li has a very large and negative triplet s-wave scattering length $a_T=-2160a_0$ [5], where a_0 is the Bohr radius, and that at sufficiently large magnetic fields a mixture of the upper two hyperfine states $|6\rangle$ and $|5\rangle$ is essentially electron-spin polarized [6].

The disadvantage of such a large triplet s-wave scattering length is that the exchange and dipolar relaxation rates for the gas are also anomalously large. Nevertheless, to suppress this decay, one can apply a magnetic bias field. In Ref. [4], we used the distorted-wave Born approximation (DWBA) to calculate the corresponding decay rate constants for these decay processes and found that, at large magnetic fields $B>10$ T, the dipolar rates are dominant, but at smaller magnetic fields, the exchange rates greatly exceed those due to the dipolar interaction. However, the DWBA is only valid at magnetic fields $B>0.1$ T, and we were at that time unable to make predictions at lower, experimentally more convenient fields.

The aim of the present paper is to provide useful information on the s-wave scattering length and exchange decay rate constants at lower magnetic fields. In view of the ongoing experiments, we will concentrate on collisions involving the following antisymmetrized hyperfine states: $|\{65\}\rangle$, $|\{64\}\rangle$, $|\{54\}\rangle$, and $|\{21\}\rangle$. The first three mixtures contain states that are low-field seeking at sufficiently high field, and therefore can be confined in a magnetic trap. In contrast, the combination $|\{21\}\rangle$ cannot be magnetically trapped, but can be confined in a far-off-resonance optical trap. We do not consider any other combination of high-field-seeking states, since the $|\{21\}\rangle$ mixture cannot decay through collisions and is therefore most favorable experimentally. In addition, van Abeelen *et al.* [7] have already considered the $|\{62\}\rangle$ combination, which is low-field seeking at very weak magnetic fields $B\leqslant 26\times 10^{-4}$ T, but does not have as large an s-wave scattering length as some other combinations [8].

To obtain the magnetic-field dependence of the s-wave scattering length and exchange decay rate constants in the various cases, we perform a full coupled-channels (CC) calculation [9], using the most up-to-date singlet and triplet potentials $V_0(r)$ and $V_1(r)$ [5]. Furthermore, we show that the rate constants and the scattering lengths found using the CC calculation can be obtained analytically using a simple approximation that we call the *asymptotic* boundary condition (ABC) approximation [10].

If the thermal energy is much smaller than the hyperfine plus Zeeman energy, $\Delta_{\alpha\beta\rightarrow\alpha'\beta'}$, gained in the transition from the incoming state $|\{\alpha\beta\}\rangle$ to an outgoing state $|\{\alpha'\beta'\}\rangle$, the corresponding exchange rate constant is given by the zero temperature expression [9]

$$G_{\alpha\beta\rightarrow\alpha'\beta'}=\lim_{k_{\alpha\beta}\rightarrow 0}\frac{\pi\hbar}{\mu k_{\alpha\beta}}|S_{\{\alpha'\beta'\}00,\{\alpha\beta\}00}(k_{\alpha\beta})-\delta_{\{\alpha'\beta'\},\{\alpha\beta\}}|^2. \quad (1)$$

In this expression, μ is the reduced mass of the two ^{6}Li atoms, $\hbar k_{\alpha\beta}$ is the relative momentum of the incoming particles in state $|\{\alpha\beta\}\rangle$, and the matrix S is the scattering matrix of the multichannel problem with angular-momentum quantum numbers $l=0$ and $m=0$. The number of channels being coupled is determined by the fact that the central interaction $V^c(r)=V_0(r)\mathcal{P}^0+V_1(r)\mathcal{P}^1$ cannot change the total nuclear plus electron-spin projection of the two-particle wave function along the magnetic field, since the operator $\mathcal{P}^S$ only projects on states with total electron spin S. So, for example, the state $|\{65\}\rangle$ can only decay to $|\{61\}\rangle$. While the nondiagonal part of the unitary S matrix gives the decay rates, the diagonal part of the S matrix gives the s-wave scattering length $a_{\alpha\beta}$ via

$$S_{\{\alpha\beta\},\{\alpha\beta\}}\rightarrow\exp(-2ik_{\alpha\beta}a_{\alpha\beta})\simeq 1-2ik_{\alpha\beta}a_{\alpha\beta}, \quad (2)$$

when $k_{\alpha\beta}\rightarrow 0$. The goal of the CC calculation is to determine the S matrix, but rather than giving a detailed description of the calculation, we refer to Ref. [9] and merely present the results here.

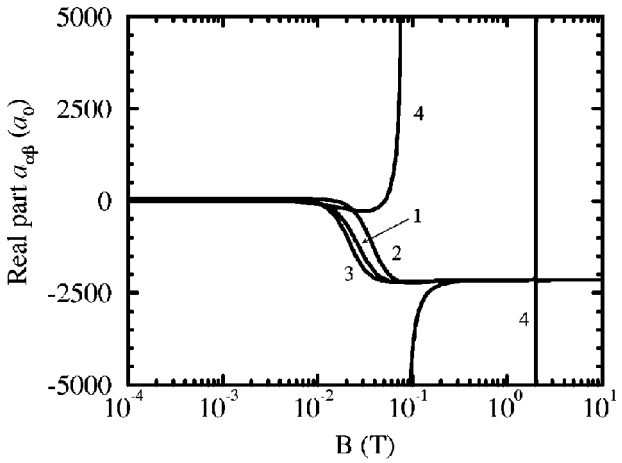

FIG. 1. Real part of zero-temperature s-wave scattering length for (1) 65, (2) 54, (3) 64, and (4) 21 collisions as a function of the magnetic field.

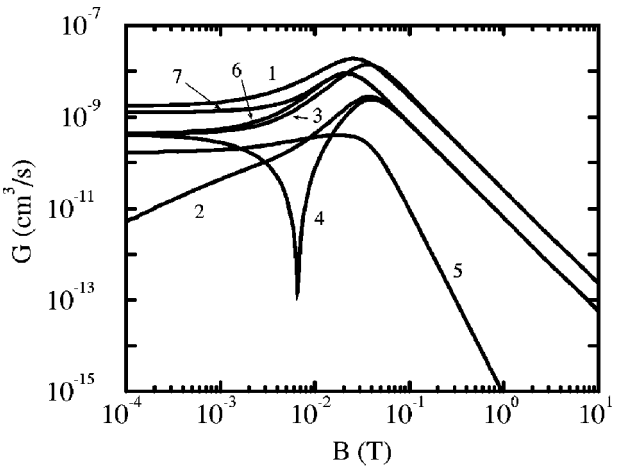

FIG. 2. Exchange decay rate constants for the processes (1) 65→61, (2) 54→63, (3) 54→52, (4) 54→41, (5) 54→21, and (6) 64→62, (7) 64→51 as a function of the magnetic-field strength.

In Fig. 1, the real part of the s-wave scattering length is plotted for the four cases of interest. Note that, in the first three cases, the s-wave scattering lengths attain the large and negative value of $a_T=-2160a_0$, only for $B\geqslant 0.05$ T. At lower magnetic fields, the scattering lengths become $47a_0$ for the first three cases, and zero in the latter case. This effect is explained in detail below. The scattering length a_{21} exhibits Feshbach resonances [11] at $B\simeq 0.08$ T and $B\simeq 1.98$ T. Physically, a Feshbach resonance arises whenever the Zeeman energy of the incoming wave function $|\{21\}\rangle$, which is almost purely triplet, coincides with a bound-state energy of the singlet potential $V_0(r)$. Only the state $|\{21\}\rangle$ can exhibit Feshbach resonances at the magnetic fields of interest since it is the only combination that has a negative total energy (about $-2\mu_e B$). The precise location of these resonances is shifted slightly due to the hyperfine coupling, but their positions can be accurately computed since the binding energies of the relevant singlet states, $v=38$ and $v=37$, are accurately calculated from the experimentally determined singlet potential [5].

The decay rate constants resulting from the CC calculation are, for all possible exchange processes, plotted in Fig. 2. The sharp minimum in the rate $G_{54\rightarrow 41}$ is a result of the fact that the matrix element $\langle\{41\}|V^c|\{54\}\rangle$ is zero if $\tan\theta_-=1/\sqrt{2}$. However, the state $|\{54\}\rangle$ still remains coupled to $|\{41\}\rangle$ through the other elements in the (5×5) coupling matrix. As a result of this interference, the rate constant is never zero, and the location of the minimum is slightly shifted from the magnetic field at which $\tan\theta_-=1/\sqrt{2}$.

The second remark regarding Fig. 2 concerns the behavior of the rate constants at large B fields where $\sin\theta_\pm\simeq\theta_\pm\propto 1/B$. Neglecting the momentum dependence of the final radial wave function, the slope of each curve is determined by the magnetic-field dependence of $\sqrt{B}|\langle\{\alpha'\beta'\}|V^c|\{\alpha\beta\}\rangle|^2$. After some algebra, one can show that for curves 2, 4, 6, and 7, the relevant matrix element is equal to $\theta_\pm(V_1-V_0)/2\equiv\theta_\pm V^{ex}/2$, which is a factor 1/2 smaller than in the cases 1 and 3. Therefore, the decay rates are a factor of 4 smaller than in the latter cases, but the slopes are identical. On the other hand, the matrix element $\langle\{21\}|V^c|\{54\}\rangle=3\theta_+\theta_- V^{ex}/2$, has an additional factor of $1/B$, resulting in a steeper slope.

A comparison of the rate constants shows that the $|\{64\}\rangle$ combination is slightly more favorable than the $|\{65\}\rangle$ combination. The total rate constant of the former combination is only half the rate constant of the latter at large magnetic fields. At $B=0.1$ T, they amount to 1.49×10^{-9} cm^3/s and 2.74×10^{-9} cm^3/s, respectively.

We now show that the CC results can be accurately reproduced using a simple analytical calculation. As a specific example, we consider the 65 case, but calculation of the other combinations is analogous. In the ABC approximation, space is divided in two regions. In the interior region $r<R$, the singlet and triplet potentials dominate, while in the outer region $r>R$, the hyperfine energies prevail. The boundary R is chosen between the point $r=R_-$ where the exchange potential $V^{ex}(r)$ is of the order of the hyperfine constant a_{hf}, and the point $r=R_+$ where the triplet and singlet potentials themselves are of order a_{hf}. In our case this is between $R_-=28a_0$ and $R_+=62a_0$, and below we will use as examples $R=40a_0$ and $R=60a_0$.

In the interior region the hyperfine splitting is neglected, so that the channel wave functions are just linear combinations of the singlet and triplet scattering wave functions, which we approximate by their asymptotic forms $A_S\sin k_{\alpha\beta}(r-a_S)$ and $A_T\sin k_{\alpha\beta}(r-a_T)$, in the limit of small momentum $k_{\alpha\beta}$. The known values of the scattering lengths are $a_S=+45.5a_0$ and $a_T=-2160a_0$, respectively [5]. In the exterior region, we neglect the central interaction V^c, so the channel wave function is a plane wave $\exp(-ik_{\alpha\beta}r)$ for the incoming channel $|\{\alpha\beta\}\rangle$, and $\widetilde{S}_{\{\alpha'\beta'\},\{\alpha\beta\}}\exp(+ik_{\alpha'\beta'}r)$ for all outgoing channels $|\{\alpha'\beta'\}\rangle$. The wave numbers $k_{\alpha'\beta'}$ depend on the energy gained by the transition to the respective outgoing channel, that is, $k_{\alpha'\beta'}=\sqrt{k_{\alpha\beta}^2+2\mu\Delta_{\alpha\beta\rightarrow\alpha'\beta'}/\hbar^2}$.

The yet unknown amplitudes A_S, A_T, and $\widetilde{S}_{\{\alpha'\beta'\},\{\alpha\beta\}}$ must be determined by imposing continuity and differentiability to the wave function in each channel at $r=R$. To do so, we need to find the precise linear combination of singlet and triplet wave function in the interior region. In terms of

the basis $|S\ M_S;I\ M_I\rangle$, where $\mathbf{S}=\mathbf{s}_1+\mathbf{s}_2$ and $\mathbf{I}=\mathbf{i}_1+\mathbf{i}_2$ are the total electron and nuclear spin of the two-atom system, respectively, we find

$$|\{65\}\rangle=\sin\theta_+|0\ 0;2\ 2\rangle+\cos\theta_+|1\ 1;1\ 1\rangle,$$

$$|\{61\}\rangle=\cos\theta_+|0\ 0;2\ 2\rangle-\sin\theta_+|1\ 1;1\ 1\rangle.$$

Evidently, for the channel wave functions we have to take linear combinations with the same coefficients; so, for example, the wave function of the $|\{65\}\rangle$ channel in the interior region becomes $\psi_{65}(r)=A_S\ \sin\theta_+\ \sin k_{\alpha\beta}(r-a_S)+A_T\cos\theta_+\ \sin k_{\alpha\beta}(r-a_T)$. It can be shown easily that the coefficients $\widetilde{S}_{\{\alpha'\beta'\},\{\alpha\beta\}}$ are related to the S matrix [9] according to

$$S_{\{\alpha'\beta'\},\{\alpha\beta\}}=-\sqrt{\frac{k_{\alpha'\beta'}}{k_{\alpha\beta}}}\,\widetilde{S}_{\{\alpha'\beta'\},\{\alpha\beta\}}. \tag{3}$$

For the case of the incoming $|\{65\}\rangle$ state, we are only interested in the constants $\widetilde{S}_{\{65\},\{65\}}$ and $\widetilde{S}_{\{61\},\{65\}}$, and therefore can eliminate the constants A_S and A_T from the 4×4 set of complex equations. The resulting 2×2 set of complex linear equations for these amplitudes can be solved in orders of k_{65}, and we find to first order in k_{65}

$$\widetilde{S}_{\{65\},\{65\}}=-1+2ik_{65}\left\{R+\frac{ik_{61}^{(0)}(R-a_S)(R-a_T)}{D(k_{61}^{(0)})}-\frac{\cos^2\theta_+(R-a_T)+\sin^2\theta_+(R-a_S)}{D(k_{61}^{(0)})}\right\}, \tag{4a}$$

$$\widetilde{S}_{\{61\},\{65\}}=\frac{2ik_{65}\ \cos\theta_+\ \sin\theta_+(a_S-a_T)}{D(k_{61}^{(0)})}, \tag{4b}$$

where $k_{61}^{(0)}=\sqrt{2\mu\Delta_{65\to61}/\hbar^2}$ and

$$D(k_{61}^{(0)})=1-ik_{61}^{(0)}[\cos^2\ \theta_+(R-a_S)+\sin^2\ \theta_+(R-a_T)].$$

Combining Eqs. (4a), (3), and (2) we find the zero-momentum s-wave scattering length a_{65}, of which the real part is plotted in Fig. 3, together with the CC curve, and the result of a degenerate internal states (DIS) approximation [9]. The inset in Fig. 3 shows the imaginary part of a_{65}.

The ABC approximation is clearly much better than the DIS approximation. To obtain the DIS result, the hyperfine level splitting is neglected, which is equivalent to setting $k_{61}^{(0)}=0$ in Eq. (4a), resulting in $\mathrm{Re}(a_{65})=a_T\cos^2\theta_+ +a_S\sin^2\theta_+$ and $\mathrm{Im}(a_{65})=0$. For hydrogen and deuterium, terms containing $k_{\alpha'\beta'}^{(0)}(R-a_{T,S})$ can indeed be neglected compared to 1 at lower magnetic fields, so that DIS is a rather good approximation in that case. However, for ^{6}Li with its anomalously large value of a_T, this is not the case, and one must then take terms of order $k_{61}^{(0)}(R-a_T)$ into account. Also, for heavier alkali-metal atoms, the DIS approximation becomes increasingly bad even at lower magnetic fields, due to the dependence of $k_{\alpha'\beta'}^{(0)}$ on the atomic mass and hyperfine constant.

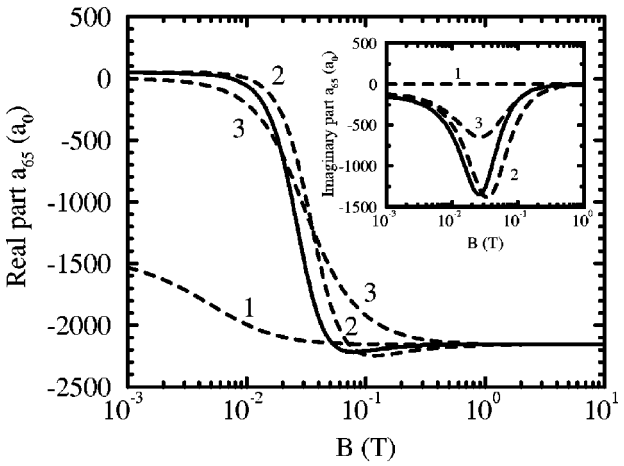

FIG. 3. Real part of the s-wave scattering length a_{65}. The solid line is the CC value, which goes to the triplet scattering length for large magnetic fields. The dashed lines are (1) the DIS approximation, (2) the ABC approximation with $R=40a_0$, and (3) the ABC approximation with $R=60a_0$. The inset shows the same for the imaginary part of a_{65}.

It is straightforward to show that, at large magnetic fields, the ABC approximation gives $\mathrm{Re}(a_{65})=a_T$ and $\mathrm{Im}(a_{65})=0$, independent of the choice of R. At $B=0$, we find $\mathrm{Re}(a_{65})=3a_S-2R\simeq57a_0$ for $R=40a_0$ and $\mathrm{Im}(a_{65})=-1/(k_{61}^{(0)}\ \tan^2\ \theta_+)\simeq-100a_0$, in surprisingly good agreement with the results of the exact CC calculation. Note that the imaginary part becomes rather large and contributes significantly to the elastic cross section $4\pi|a_{65}|^2$ at lower magnetic field.

Similarly, one can find the decay rate constant $G_{65\to61}$ from Eq. (4b) combined with Eqs. (3) and (1). The results are plotted in Fig. 4. Again, agreement with the exact CC calculation is very good, whereas the DIS approximation is in error by several orders of magnitude. We also worked out

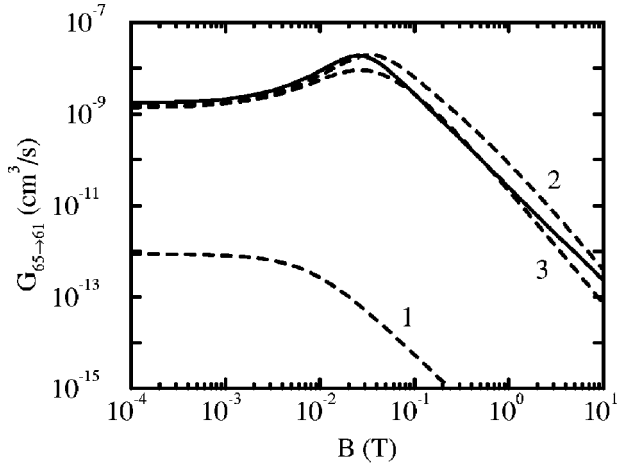

FIG. 4. Exchange decay rate $G_{65\to61}$ of the ^{6}Li gas. The solid line gives the CC result. The dashed lines represent (1) the DIS approximation, (2) the ABC approximation with $R=40a_0$, and (3) the ABC approximation with $R=60a_0$.

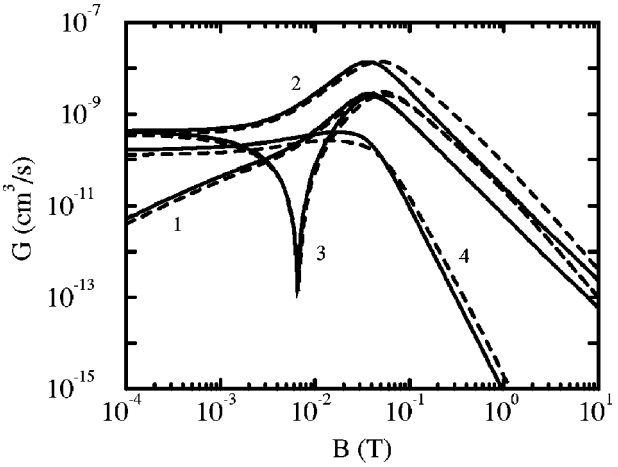

FIG. 5. Comparison of the CC calculation (solid lines) and the ABC approximation with $R=40a_0$ (dashed lines) for the exchange decay rate constants of the processes (1) 54→63, (2) 54→52, and (3) 54→41, (4) 54→21.

the field-dependent scattering lengths and exchange rate constants corresponding to the other three hyperfine mixtures using the ABC approximation. In these cases, the set of complex equations is greater than 4×4, and a completely analytic treatment is more involved. Therefore, we solved the equations numerically. In all cases, we find good agreement between the ABC approximation and the exact CC calculation. As an example, the ABC approximation for the decay rate constants in the 54 case is plotted in Fig. 5, using $R=40a_0$.

We thus conclude that the ABC approximation can easily give an accurate estimate of the collisional properties of interest, whereas the DIS approximation can be off by many orders of magnitude. We believe that this is also true for other alkali-metal atoms. Alternatively, Verhaar *et al.* describe a CC method where the inner region $r<r_0$ of the singlet and triplet potentials is described by the accumulated phases at the boundary $r=r_0<R_-$, and the collisional quantities are obtained by integrating Schrödinger's equation in the outer region $r>r_0$ using the exact potentials [12]. In contrast, the ABC approximation requires no integration and no explicit knowledge of the potentials other than the scattering lengths [13]. Of course, the results will vary slightly with the actual choice of R. It is difficult to predict *a priori* which R reproduces the exact results for an arbitrary atom best, but any R chosen as indicated previously, will give at least a good order-of-magnitude estimate.

We acknowledge useful discussions with Jean Dalibard, Marc Mewes, and John Tjon. The work at Rice was supported by the National Science Foundation, NASA, the Texas Advanced Technology Program, and the Welch Foundation.

[1] M. H. Anderson *et al.*, Science **269**, 198 (1995).

[2] C. C. Bradley *et al.*, Phys. Rev. Lett. **75**, 1687 (1995); C. C. Bradley, C. A. Sackett, and R. G. Hulet, *ibid.* **78**, 985 (1997).

[3] K. B. Davis *et al.*, Phys. Rev. Lett. **75**, 3969 (1995).

[4] H. T. C. Stoof *et al.*, Phys. Rev. Lett. **76**, 10 (1996); M. Houbiers *et al.*, Phys. Rev. A **56**, 4864 (1997).

[5] E. R. I. Abraham *et al.*, Phys. Rev. A **55**, R3299 (1997).

[6] The six hyperfine states of the internal Hamiltonian $H_{int}=(a_{hf}/\hbar^2)\mathbf{s}_e\cdot\mathbf{i}_n+(2\mu_e\mathbf{s}_e/\hbar-\mu_n\mathbf{i}_n/\hbar)\cdot\mathbf{B}$ of the ^{6}Li atom are given by $|1\rangle=\sin\theta_+|1/2\ 0\rangle-\cos\theta_+|-1/2\ 1\rangle$, $|2\rangle=\sin\theta_-|1/2\ -1\rangle-\cos\theta_-|-1/2\ 0\rangle$, $|3\rangle=|-1/2\ -1\rangle$, $|4\rangle=\cos\theta_-|1/2\ -1\rangle+\sin\theta_-|-1/2\ 0\rangle$, $|5\rangle=\cos\theta_+|1/2\ 0\rangle+\sin\theta_+|-1/2\ 1\rangle$, $|6\rangle=|1/2\ 1\rangle$, in increasing order of energy, with $|m_s m_i\rangle$ the projection of the electron and nuclear spin, and $\sin\theta_\pm=1/\sqrt{1+(Z^\pm+R^\pm)^2/2}$, $Z^\pm=(\mu_n+2\mu_e)B/a_{hf}\pm1/2$, and $R^\pm=\sqrt{(Z^\pm)^2+2}$.

[7] F. A. van Abeelen, B. J. Verhaar, and A. J. Moerdijk, Phys. Rev. A **55**, 4377 (1997).

[8] The s-wave scattering length of the $|\{62\}\rangle$ combination is about $-1615a_0$, for $B\leqslant26\times10^{-4}$ T.

[9] H. T. C. Stoof, J. M. V. A. Koelman, and B. J. Verhaar, Phys. Rev. B **38**, 4688 (1988), and references therein.

[10] See H. Feshbach, *Theoretical Nuclear Physics—Nuclear Reactions* (John Wiley & Sons, New York, 1992), p. 226, for a discussion of the boundary condition model.

[11] E. Tiesinga, B. J. Verhaar, and H. T. C. Stoof, Phys. Rev. A **47**, 4114 (1993).

[12] B. J. Verhaar, K. Gibble, and S. Chu, Phys. Rev. A **48**, R3429 (1993).

[13] Since the method can by analytic continuation also deal with closed channels, it reproduces the correct Wigner threshold laws [P. S. Julienne and F. H. Mies, J. Opt. Soc. Am. B **6**, 2257 (1989)], and because it is nonperturbative in the hyperfine interaction, it can also approximately deal with the first Feshbach resonance.